*Bangladesh Journal of Physics, Vol. **28**, Issue 2, pp. 51-58, December 2021*

MICROSTRUCTURE AND MAGNETIZATION PROCESS DUE TO CD^{2+} DOPED Ni-Mg SPINEL FERRITES

ZAKIYA SULTANA[1], M. A. HOSSAIN[1], S. K. SHIL[1], RIMI RASHID[2], M. N. I. KHAN[2] AND S. S. SIKDER[1]

[1]*Department of Physics, Khulna University of Engineering & Technology, Khulna, Bangladesh*
[2]*Materials Science Division, Atomic Energy Centre, Dhaka, Bangladesh*

[*]*Corresponding author e-mail: liton@phy.kuet.ac.bd*

Received on 24.07.2021, Revised received on 18.06.2021, Accepted for publication on 21.11.2021

DOI: https://doi.org/10.3126/bjphy.v28i2.78683

ABSTRACT

The $Ni_{0.5}Mg_{0.5}Cd_xFe_{2-x}O_4$ ferrites (x = 0.00, 0.02, 0.04, 0.06, 0.08, and 0.10) were prepared by the solid-state reaction method using laboratory-grade oxide materials. Samples from each composition were prepared and then sintered at 1000 °C for 3 hours. The Cd-doped Ni-Mg ferrites' structural and surface morphology effects were analyzed by XRD and SEM. XRD analysis indicated that all the sintered samples crystallized in a single-phase cubic spinel structure. It follows from Vegard's law that, in Ni-Mg-Cd ferrites, the lattice parameter increased linearly with the substitution of Fe^{3+} ions by Cd^{2+}. In all the samples, the theoretical density was higher than their bulk densities due to the pores present in them, as the sintering temperature is influenced. SEM images showed that the Cd-doped Ni-Mg ferrites significantly modified the average grain size; thus, the surface morphology appeared to be homogeneous and consisted of well-defined spherical grains. The average grain size decreased while doping with Cd^{2+} in $Ni_{0.5}Mg_{0.5}Cd_xFe_{2-x}O_4$ up to x = 0.08 and then increased with a further increase in doping concentration. No significant effect on M_s, H_c, and M_r was observed while measuring from the *M-H* curve by VSM and hysteresis loops. The coercive value H_c was very low, and hence Ni-Mg-Cd ferrites belong to the family of soft ferrites. The M_s value increased in all samples with the content of Cd doping. With these results, it can be asserted that the addition of Cd can make Ni-Mg ferrites more magnetic at the core and change their structure, along with surface appearance; thus, these materials will be useful in many magnetic applications.

Keywords: *Ferrites, XRD, SEM, Grain size, Coercive, Magnetization*

1. INTRODUCTION

Ni-Cd ferrites are among the most important materials applied in microwave applications because of their high coercivity (H_c), remanence (M_r), and saturation magnetization (M_s). Nowadays, Cd-doped ferrites are being considered for academic research and engineering as promising materials. The inclusion of small Cd ions into ferrite samples leads to significant changes in their magnetic, transport, and structural properties, depending on the type of electrical components used - most of them behave like ferrimagnetic materials [1-4].

Nickel ferrite represents the partially inverse spinel family and is widely used in electronic and microwave devices due to its high electrical resistivity and dielectric losses [5-6]. The structural, magnetic, and optical properties of Ni-Mg-Zn ferrite prepared by using different complex agents via the sol-gel method were studied, and it was observed that XRD showed all major peaks related to the spinel structure without additional peak intensity [7]. The research on doping of Ni^{2+} on magnesium ferrite nanoparticles of composition $Ni_xMg_{1-x}Fe_2O_4$ (x = 0, 0.25, 0.5, 0.75, and 1) showed a spinel cubic structure and a single phase. FESEM analysis indicated that all samples were

composed of spinel crystalline particles [8]. Further investigations into the structural and magnetic properties of Ni-Mg-Co spinel ferrite nanoparticles sintered at different temperatures confirmed that the sintered samples exhibited the highest saturation magnetization (59.03 emu/g), remanent magnetization (30.65 emu/g), and squareness (0.519). The increasing peak height in their XRD patterns indicated the cubic spinel structure and good crystalline and magnetic stability of these samples [9]. Cd-substituted Ni-Mg ferrites belong to a group of the most important magnetic materials owing to their highest permeability, very small hysteresis losses, constancy of properties over the widest temperature range, and low core losses at high-frequency applications. Their properties largely depend on both microstructure features. This study reports the structural and magnetic effects of the substitution of non-magnetic Mg^{2+} ions by magnetic Ni^{2+} ions in different ferrite samples. It was found that a sharp rise in initial permeability at x = 0.3 exists for the $Ni_xMg_{0.5-x}Cu_{0.1}Zn_{0.4}Fe_2O_4$ ferrite [10-11].

It is expected that the structural and magnetic properties of Ni-Cd ferrites will show significant changes upon substitution of Mg^{2+} ions in the nanoferrite system. There has been little research carried out on Cd doping in Ni-Mg ferrites. There are a number of challenges associated with doping RE ions into ferrites, including limited solubility and ambiguous effects on electrical and magnetic properties. The role of RE Cd^{2+} ion doping in Ni-Mg ferrite reflects multiple magnetic phases at different sintering temperatures and magnetic fields. In this work, the impact of Cd^{2+} ions substitution for Fe^{2+} ions in Ni-Mg ferrite on their structural and magnetic properties is studied.

2. EXPERIMENTAL DETAILS

The sample of mixed ferrites with various compositions has been prepared by the solid-state reaction method by keeping ionic radial and maintaining charge neutrality of this composition. In this research, Cd-substituted Ni-Mg ferrites with compositions $Ni_{0.5}Mg_{0.5}Cd_xFe_{2-x}O_4$ are synthesized, characterized, and investigated. High-purity powders of NiO (99.9%), MgO (99.9%), CdO (99.9%), and Fe_2O_3 (99.9%) as raw materials. The exact amounts of compounds were calculated for each composition. The used raw materials were weighed and mixed thoroughly by hand milling. At constant time of hand milling, a few drops of acetone were added to increase the degree of mixing. The slurry is dried, and the powder is pressed into a disc shape after pre-sintered mixture at 850 ºC for 4 hours. The pre-sintered samples are crushed, and subsequently, hand milling in distilled water reduces the small, uniform crystalline size from calcined powder into fine powders. From the fine powders, the disk-shaped samples were prepared and sintered at 1000 ºC for 3 hours. After sintering, the sample got the expected product and then studied the magnetic properties of this desired ferrite sample. For sintering our samples, we used the KSL-1700X-S Furnace from Solid State Physics Lab, KUET. The samples were sintered at 1000 ºC for 3 hours. In this work, we used the Phillips X'pert PRO X-ray diffractometer of the Atomic Energy Centre, Dhaka. The wavelength of the used X-ray is (λ = 1.5418 Å) and is of the same order of magnitude as that of the lattice constant of crystals, and this makes it so useful in structural analysis of the crystal structure of the sample. The surface morphology of the samples is investigated using various microstructures, which means grain size is affected by varying sintering temperatures using an SEM, Center of Excellency, Dhaka University, Dhaka. Magnetization properties of the samples have been measured as a function of field using VSM and analyzing hysteresis parameters from field-dependent magnetization, material science division, BAEC, Dhaka.

3. RESULTS AND DISCUSSIONS

3.1 Crystalline phase identification through XRD data analysis:

The phase formation behavior of the Cd^{2+} ion-doped $Ni_{0.5}Mg_{0.5}Cd_xFe_{2-x}O_4$ ferrites sintered at 1000 °C for 3 h as a function of Cd doping concentration (x = 0.00, 0.02, 0.04, 0.06, 0.08, 0.10) was analyzed using XRD, and is represented in Fig. 1. The XRD spectra depicted good crystallization with well-defined diffraction peaks even without the doping of Cd^{2+} ions in Ni-Mg ferrites. Cd^{2+} ion doping into the Ni-Mg ferrites indicated good crystallization with well-defined diffraction lines indexed to the *fcc* spinel structure.

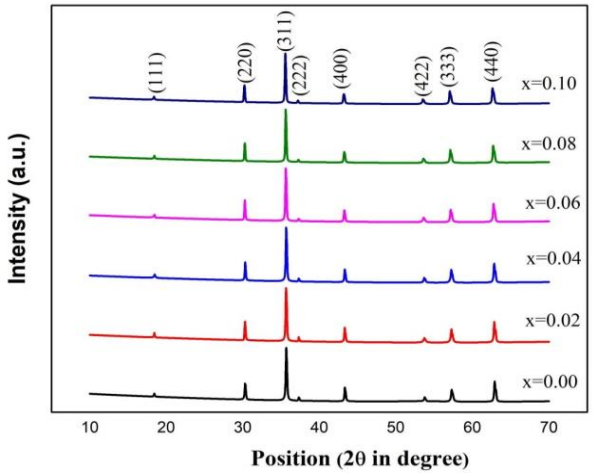

Fig. 1. XRD spectra of $Ni_{0.5}Mg_{0.5}Cd_xFe_{2-x}O_4$ [where x = 0.00, 0.02, 0.04, 0.06, 0.08 and 0.10] ferrites sintered at 1000 °C holding time 3 hours.

Table 1: Data of the lattice parameter (*a*), X-ray density (ρ_x), bulk density (ρ_B) and porosity (*P*%) of $Ni_{0.5}Mg_{0.5}Cd_xFe_{2-x}O_4$ ferrites sintered at 1000 °C for 3 hrs.

Content	*a* (Å)	ρ_x (gm/cm^3)	ρ_B (gm/c^3)	Porosity (%)
x = 0.00	8.349	4.96	2.79	43.57
x = 0.02	8.354	4.98	2.67	46.42
x= 0.04	8.356	4.99	2.66	46.68
x = 0.06	8.362	5.01	2.64	47.33
x = 0.08	8.365	5.03	2.53	49.75
x = 0.10	8.376	5.04	2.56	49.20

The lattice parameters of all the samples have been precisely determined using Nelson Relay Function F(θ) [12] in equation $F(\theta)=\frac{1}{2}\left[\frac{\cos^2\theta}{\sin\theta}+\frac{\cos^2\theta}{\theta}\right]$ considering all the XRD reflections.

These experimental results indicate that the lattice parameter of Ni-Mg-Cd ferrites, $Ni_{0.5}Mg_{0.5}Cd_xFe_{2-x}O_4$, increases linearly with the substitution of Fe^{3+} ions by Cd^{2+} ions, which follows Vegard's law. This increase in the lattice parameter is attributed to the substitution of the smaller Fe^{3+} ions from the tetrahedral (A) sites to the octahedral (B) sites by the larger Cd^{2+} ions, as

illustrated in Table 1. The bulk density of the ferrite samples is lower than the X-ray density due to the presence of pores formed during the preparation and sintering processes.

While increasing the Cd content, porosity increases monotonically in samples. These porosities are very difficult to get rid of completely, as they are partly due to the evaporation of the constituents, especially Mg^{2+} ions, during sintering. At higher sintering temperatures, density decreases due to increased intragranular porosity caused by discontinuous grain sizes [13]. The structural properties have a big influence on the magnetic properties, that is, complex permeability and flux density

3.2 Microstructure analysis by SEM images analysis:

Micrographs show that dense microstructures are obtained for all ferrite samples, with an average grain size measured from the SEM images using the linear intercept method. Fig. 2: SEM microstructure of $Ni_{0.5}Mg_{0.5}Cd_xFe_{2-x}O_4$ ferrite pellets sintered at 1000°C for 3 hours. The average grain sizes calculated by ImageJ software from SEM micrographs are given in Table 2. The densification of sintered ferrites is assisted by a liquid phase formed due to capillary forces. This behavior reflects the competition between the driving force of grain boundary movement and the retarding force exerted by pores [14]. The microstructure of Ni-Mg-Cd ferrite is clearly influenced by the concentration of Cd^{2+} ions replacing Fe in the ferrite.

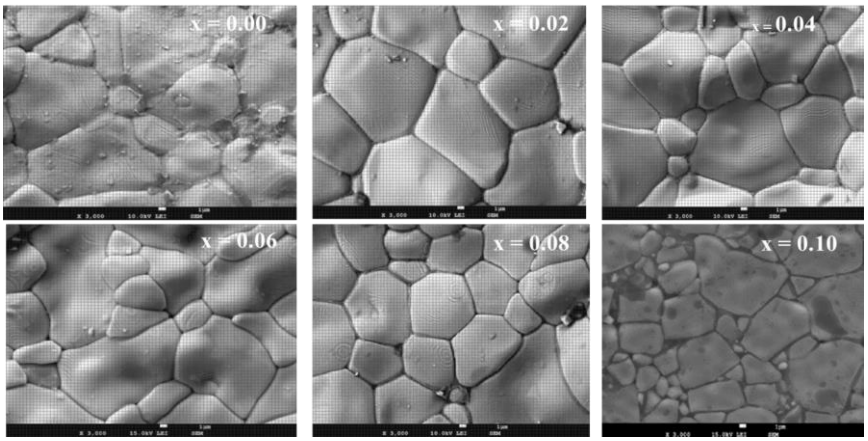

Fig. 2: SEM micrograph of $Ni_{0.5}Mg_{0.5}Cd_xFe_{2-x}O_4$ferrites sintered at 1000°C for 3 hours.

Table 2: Average grain size of $Ni_{0.5}Mg_{0.5}Cd_xFe_{2-x}O_4$ [where x = 0.00, 0.02, 0.04, 0.06, 0.08 and 0.10] ferrites sintered at 1000ºC for holding time 3 hours.

Name of the sample	Contents	Average grain size (μm)
$Ni_{0.5}Mg_{0.5}Fe_2O_4$	x = 0.00	11.64
$Ni_{0.5}Mg_{0.5}Cd_{0.02}Fe_{1.98}O_4$	x= 0.02	14.53
$Ni_{0.5}Mg_{0.5}Cd_{0.04}Fe_{1.96}O_4$	x = 0.04	13.55
$Ni_{0.5}Mg_{0.5}Cd_{0.06}Fe_{1.94}O_4$	x = 0.06	11.67
$Ni_{0.5}Mg_{0.5}Cd_{0.08}Fe_{1.92}O_4$	x = 0.08	11.09
$Ni_{0.5}Mg_{0.5}Cd_{0.10}Fe_{1.90}O_4$	x = 0.10	11.38

Figure 2 (x = 0.00) depicts a monophasic homogeneous microstructure without Cd content. In addition, the Cd-doped Ni-Mg ferrites as illustrated in Fig. 2 (x = 0.02, 0.04, 0.06, 0.08, and 0.10) present biphasic homogeneous microstructures consisting of dark ferrite matrix grains and small whitish grains at grain junctions and boundaries. It shows a maximum grain size of the matrix phase for x = 0.02 and comparatively smaller for the composition x = 0.08; the average estimated grain size varies from 11.09 μm to 14.53 μm. Therefore, the increase in Cd^{2+} ion content in Ni-Mg ferrites leads to a decrease in grain size, indicating that the microstructure of these ferrites strongly depends on the amount of Cd^{2+} ions, especially at higher sintering temperatures.

In Fig. 2, the presence of a monophasic homogeneous microstructure without Cd^{2+} ions is observed. Additionally, Cd-doped Ni-Mg ferrites depicted in Fig. 2 have biphasic homogeneous microstructures composed of dark ferrite matrix grains and small whitish grains at grain junctions and boundaries. The grain size of the matrix phase is at its maximum, 15.74 μm, for x = 0.00, and is relatively smaller for Cd-doped Ni-Mg ferrites sintered at 1000°C for 3 hours. With the addition of Cd content, the average grain size initially decreases and then increases at x = 0.0.

However, the crystal grain growth depends on grain boundaries migrating and larger crystal grains swallowing the small ones. It facilitates the grain growth by increasing the rate of cation inter diffusion as a result of its segregation to the grain boundaries. The driving force of the grain boundary in each grain is homogeneous; the sintered body attains a uniform grain distribution. Abnormal grain growth occurs when the driving force is inhomogeneous. The strength of the driving force depends upon the diffusivity of individual grains, sintering temperature, and porosity. The surface morphology is found to be changed from granular to lamellar due to Cd^{2+}-ion-doped Ni-Mg ferrites. Finally conclude that from Table 3, those Ni-Mg-Cd ferrites sintered at 1000 °C/3 hrs show a homogeneous microstructure with an average grain size of about 8 μm, more stable, and a uniform distribution.

3.3 Magnetization measurement analysis:

The hysteresis loops show no noticeable effects, and all samples exhibit low coercive values (H_c), indicating that both Cd-doped and undoped Ni-Mg ferrites belong to the family of soft ferrites. The nature of these magnetization curves is linked to the soft magnetic behavior of Cd-doped Ni-Mg ferrites. The magnetization (M) of all ferrites increases linearly with the applied magnetic field (H).

The room temperature magnetic hysteresis graphs of $Ni_{0.5}Mg_{0.5}Cd_xFe_{2-x}O_4$, ferrites are sintered at 1000 °C for 3 hours and have been measured at room temperature up to 10 kOe magnetic field (H) and presented in Fig. 3**,** respectively.

Table 3: The values of M_s, H_c, M_r and M_r/M_s of $Ni_{0.5}Mg_{0.5}Cd_xFe_{2-x}O_4$ ferrites sintered at 1000 °C for holding time 3 hours.

Content	M_s (emu/g)	H_c (Oe)	M_r (emu/gm)	M_r/M_s
x = 0.00	29.50	70.5	0.04	0.004
x = 0.02	30.10	74.5	0.50	0.02
x = 0.04	31.72	102.2	5.30	0.17
x = 0.06	38.60	98.8	6.50	0.17
x = 0.08	42.23	19.0	0.25	0.006
x = 0.10	46.59	78.0	4.90	0.11

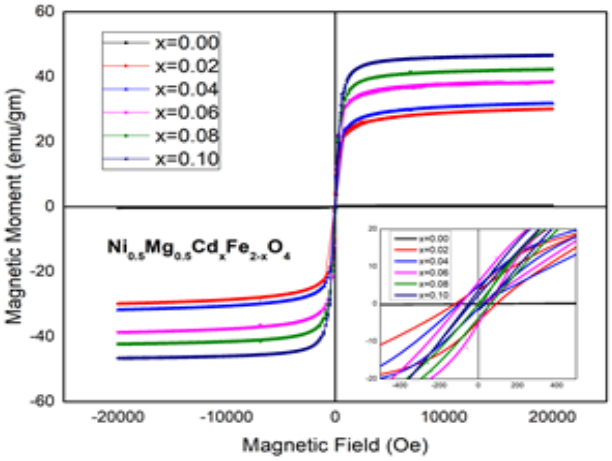

Fig. 3: The room temperature magnetic hysteresis graphs of $Ni_{0.5}Mg_{0.5}Cd_xFe_{2-x}O_4$, ferrites are sintered at 1000°C for 3 hours and have been measured at room temperature up to 10 kOe magnetic field (H) and presented in Fig. 3, respectively.

In Table 3, the value of H_c is found to gradually increase up to x = 0.04 with increasing Cd ions, and after that, H_c decreases from x = 0.06 to x = 0.08 and then increases again at x = 0.10. These are reasons, the movement of domain walls has become more difficult, and hence H_c increases and decreases mean which distinguishes reversible and irreversible relaxation due to Cd^{2+} ions. Irreversible types of relaxation are compared to an atomic pair that corresponds to irreversible domain wall movements under an external field. The M_r values are found to increase up to x = 0.06 after decreases to x = 0.08 and again increase to x = 0.10. These increase and decrease in nature due to the random canted model; substitution of nonmagnetic Cd cations in one sublattice of ferrimagnetic Fe^{3+} ions lead to spin canting in the other sublattice, resulting in decreased nature in total magnetization per unit formula. The variation of M_r/M_s with respect to the addition of Cd^{2+} ions is also shown in Table 3 for better convenience. Table 3 shows that saturation magnetizations increase with the rising Cd^{2+} ion content due to improved density and higher permeability of Cd-doped Ni-Mg ferrites. The value of M_s is nominal, with all Cd-doped compositions exhibiting higher values than undoped Ni-Mg ferrite. This may be attributed to the increased density in the initial stage of Cd-doped Ni-Mg ferrite, resulting from the enhancement of the sublattice magnetic moment.

The coercivity value of H_c for Cd-doped Ni-Mg ferrites is generally lower than that of undoped samples, except for the maximum value at x = 0.10. This is because of increased difficulty in domain wall movement, giving rise to higher H_c values and making a distinction between reversible and irreversible relaxation types caused by Cd^{2+} ions. The M_r value increases gradually in the Ni-Mg ferrites with the addition of Cd^{2+} ions, perhaps due to the replacement of magnetic Fe^{3+} ions with nonmagnetic Cd^{2+} ions. Table 3 also presents the variation of M_r/M_s with respect to the addition of Cd content. At higher sintering temperatures, the rate of increase for M_s and H_c becomes very low, which is perhaps due to the porosity of the ferrite sample and the formation of a second phase. H_c is a microstructural property that is dependent on the defects, strains, and non-magnetic atoms in the material [15]. The observed increasing trends of H_c have been attributed to the presence of nonmagnetic Cd^{2+} ions along with favorable microstructure in Ni-Mg ferrites, which may also include sufficient defects

4. CONCLUSIONS

XRD characterizations confirm the single-phase spinel structure of Ni-Mg-Cd ferrites, which is quite free from ambiguity in the spinel structures. The bulk density is lower than the X-ray density due to the pores formed in the preparation and sintering processes. With an increase in Cd content, monotonic increase of porosity is observed at 1000°C, and complete removal of such pores is not possible due to the evaporation of the constituents, especially Mg^{2+} ions, in these ferrites. SEM micrographs show that the grain size of the matrix phase for x = 0.00 is the largest, at 15.74 μm, with a relative decrease in grain size for Cd-doped Ni-Mg ferrites sintered at 1000°C for 3 hours. Because of the homogeneous driving force at the grain boundaries, the grains distribute uniformly within the sintered body. The Ms for all the samples increases as the doping content of Cd increases. This increase in Ms is due to the dilution of magnetic moment at the tetrahedral A-site through the Cd^{2+} ion substitutions that align parallel to the octahedral B-site magnetization since there are twice as many cations on B-sites compared to A-sites. Hysteresis loops display low Hc increases, indicating that there lies a difference between reversible and irreversible relaxation types due to Cd^{2+} ions. In Ni-Mg ferrites, as the magnetic Fe^{3+} ions are replaced by nonmagnetic Cd^{2+} ions, the value of remanent magnetization, Mr, increases gradually.

ACKNOWLEDGEMENTS

The authors are thankful to the Department of Physics, Khulna University, Bangladesh; and Atomic Energy Centre, Bangladesh for their valuable assistance in completing the research.

REFERENCES

[1] M. B. H. Hamida, T. Mzoughi and N. Hamdaoui Improvement of Magnetic and Dielectric Properties Through Cd Substitution in Mg–Ni Spinel Ferrite. Journal of Inorganic and Organometallic Polymers and Materials, 1-18 (2024).

[2] H. Yang, X. Yang, J. Lin, F. Yang, Y. He, and Q. Lin. Effect of Cd^{2+} substitution on structural–magnetic and dielectric properties of Ni–Cu–Zn spinel ferrite nanomaterials by Sol–Gel. Molecules, 28, 16 (2023), 6110.

[3] N. Amin, A. Razaq, A. U., Rehman, K. Hussain, M. A. U. Nabi, N. A. Morley and S. Amin. Transport properties of Ce-doped Cd ferrites $CdFe_{2-x}Ce_xO_4$. Journal of Superconductivity and Novel Magnetism, 34 (2021), 2945-2955.

[4] A. N. M. Farea, S. Kumar, K. M. Batoo, A. Yousef, and C. G. Lee. Structure and electrical properties of $Co_{0.5}Cd_xFe_{2.5-x}O_4$ ferrites. Journal of Alloys and Compounds, 464(1-2), 361-369 (2008).

[5] M. D. Hossain, M. A Hossain, and S. S. Sikder. Hysteresis loop properties of rare earth doped spinel ferrites: A review. Journal of Magnetism and Magnetic Materials, 564 (2022), 170095.

[6] M. D. Hossain, M.S. Hossain, M. A. Hossain, M. N. I. Khan, S.S. Sikder). Finding the best frequency dependent performance of 3d transition metals (Co, Ni, and Mn) substituted nano magnetite for miniaturizing device applications. Ceramics International. Ceramics International 50, no. 22 (2024): 45813-45824.

[7] Y. Zhang, A. Sun and Z. Suonan. The structural, magnetic, and optical properties of Ni–Mg–Zn ferrite prepared with different complexing agents via sol–gel method. Journal of Materials Science: Materials in Electronics, 32 (2021), 13350-13368.

[8] N. S. Kumar, N. Das, K. Devlal, S. Seema, M. S. Shekhawat, M. Hidayath and S. A. Khader. Dielectric and magnetic studies of Ni-Mg mixed ferrite by combustion method. In AIP Conference Proceedings Vol. 2220, No. 1 (2020). AIP Publishing.

[9] X. Zhao, A. Sun, W. Zhang, L. Yu, Z. Zuo, N. Suo, and Y. Han. Studies on structural and magnetic properties of Ni-Mg-Co spinel ferrite nanoparticles sintered at different temperatures. Modern Physics Letters B, 34, 03 (2020), 2050041.

[10] S. G. Bachhav, A. A. Patil, and D. R. Patil. Electric and Dielectric Properties of Ni Substituted Mg-Zn-Cu Ferrites. Advances in Ceramic Science and Engineering, 2, 2 (2013), 89-94.

[11] S. G. Bachhav, R. S. Patil, P. B. Ahirrao, A. M. Patil and D. R. Patil. Microstructure and magnetic studies of Mg–Ni–Zn–Cu ferrites. Materials Chemistry and Physics, 129, 3 (2011), 1104-1109.

[12] K.T. Jacob, S. Raj, and L. Rannesh. Vegard's law: a fundamental relation or an approximation? International Journal of Materials Research, 98, 9 (2007), 776-779.

[13] S. Akhter, S. M. Hoque and M. A. Hakim. Effect of sintering temperature on structural and magnetic properties of bulk Mg-ferrites. International Journal of Materials Research, 110, 10 (2019), 979-984.

[14] S. S. Bellad, S. C. Watawe and B. K. Chougule. Microstructure and permeability studies of mixed Li-Cd ferrites. Journal of magnetism and magnetic materials, 195, 1(1999), 57-64.

[15] Z. Babasafari, A. V. Pahlevani, F., Kong, C. Du, M., Toit and R. Dippenaar. Effect of Microstructural Features on Magnetic Properties of High-Carbon Steel. Metallurgical and Materials Transactions A, 52 (2021), 5107-5122.